

Investigation of Temperature-dependence of Block Copolymer Poly(isoprene)-*b*-poly(ethylene oxide) Nanostructure

Kristjan Kunnus
supervisor: Andreas Timmann

September 14, 2007

Abstract

The structural changes of poly(isoprene)-*b*-poly(ethylene oxide) (PI-PEO) were studied during the heating from the temperature 28 °C (ambient temperature) up to 80 °C. In addition the structures in room temperature before and after heating are compared. Four samples with different water concentration were investigated. For characterizing the samples small-angle x-ray scattering (SAXS) at the beamline BW4 at the DORIS III storage ring were used.

1 Introduction

1.1 Structure of amphiphilic block copolymers

Block copolymers are special kind of copolymers made up of blocks of different polymerized monomers. If block copolymer has two blocks, then its called a diblock copolymer. Special case of block copolymers are amphiphilic block copolymers (ABC's) consisting of polymer blocks with different cohesion energies (e.g., diblock copolymer with one block hydrophilic and second hydrophobic). ABC's has interesting phase behavior called a microphase separation. If the molecular forces between same blocks of different molecules are stronger then between different blocks, then it is energetically favorable that hydrophilic blocks form one phase and hydrophobic blocks form other phase (in case of diblock ABC's). But because different blocks of the same

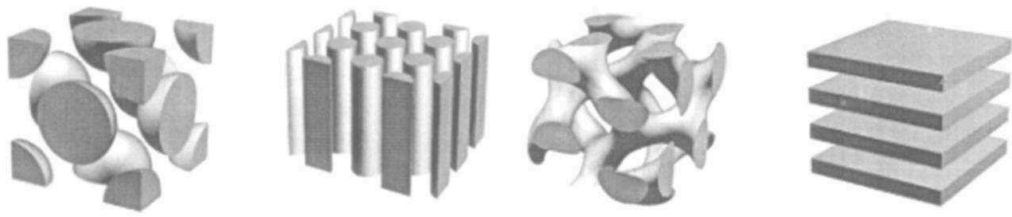


Figure 1: Nanostructures of ABC's: fcc spheres, hexagonally packed cylinders, bicontinuous double diamond morphology and lamellae.

molecule are covalently bonded the two phases can't separate macroscopically and they form nanometer-sized structures. The typical structures of ABC's are seen in figure 1¹. The concrete structure of ABC depends on several parameters [1], the most important are:

1. f , the volume fraction of one phase;
2. N , the degree of polymerization (total number of monomers in a molecule);
3. χ , Flory-Huggins interaction parameter, describes the polymer/polymer and polymer/solvent interactions.

In case of certain ABC, there is possible to modify the structure with changing the χ trough altering the temperature or by adding a selective solvent (for example water), what changes both the f and χ .

1.2 X-ray scattering from matter

When materials are exposed to x-rays (electromagnetic radiation with a wavelength in the range of 10 to 0.01 nm) several primary processes can take place:

1. photoelectron production;
2. inelastic (Compton) scattering;
3. electron-positron pair production;
4. elastic scattering from free electrons (Thomson scattering; electrons are not free inside the material, but frequency of the x-ray wave is so large, that they act as free).

¹Picture taken from <http://www.sfu.ca/physics/research/workarea/frisken/>

SAXS is based on Thomson scattering and in this case the energy (wavelength) of the incident photon is conserved and only its propagating direction is changed. Relations between incidence and scattered wavevectors (\vec{k}_0 and \vec{k} respectively) are:

$$|\vec{k}_0| = |\vec{k}| \quad (1)$$

$$\vec{k}_0 + \vec{q} = \vec{k} \quad (2)$$

Equation 2 is a definition of scattering vector \vec{q} . Differential scattering cross section of a single free electron for unpolarized incident radiation is:

$$\frac{d\sigma}{d\Omega} = r_e^2 \frac{1 + \cos^2(2\theta)}{2} \quad (3)$$

here r_e is classical electron radius ($r_e = \frac{e^2}{4\pi\epsilon_0 m_e c^2} \approx 2.8 \cdot 10^{-15} m$) and 2θ is scattering angle (angle between primary and scattered beam).² Because of the factor r_e^2 scattering is a very weak process. The intensity depends only slightly on the 2θ , which is practically constant for the small angles.

Photons are scattered from the electrons (because nuclei are very heavy compared to electrons) and so the material is described by electron density distribution function $\rho(\vec{r})$, where \vec{r} is position vector. Because of the specific electron density differences inside a every material the resulting angular distribution of scattered radiation is characteristic to material and represents its spatial structure. To quantitatively describe elastic x-ray scattering, one can to following simplifications:

- only photons of the primary beam are scattered (no secondary scattering);
- x-rays are treated as a scalar waves (ignoring the polarization);
- only the wave's spatial dependence is considered.

Taking these simplifications into account, it is possible to show that:

$$I = |A(\vec{q})|^2 \quad (4)$$

$$A(\vec{q}) = A_e \int_V \rho(\vec{r}) e^{-i\vec{q}\vec{r}} d^3r \quad (5)$$

where A_e denotes the scattering amplitude of one electron, $A(\vec{q})$ is the scattering amplitude of material and integration is over the whole volume of

²Differential scattering cross section is related to scattering intensity trough equation: $I = I_0(\frac{1}{4\pi L^2})(\frac{d\sigma}{d\Omega})$, where I_0 is intensity of incident wave and L is distance to observation point.

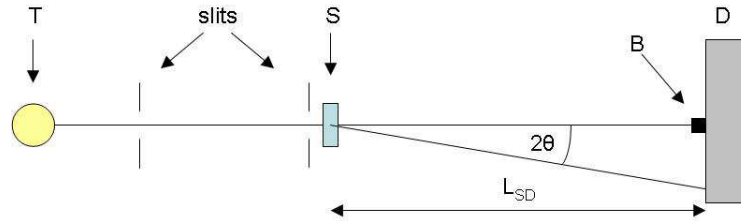


Figure 2: Principle of the SAXS experiment in transmission geometry . The drawing shows the monochromatic x-ray source T, the sample S, the beam-stop B, the detector D and the slits used to define the incident beam. L_{SD} is the sample-detector distance and 2θ is scattering angle.

material [2]. In most cases there is very rational to describe crystal structure not as continuous function $\rho(\vec{r})$, but instead of that as a ordered set of particles (atoms, molecules, nanoparticles). Then it is useful to introduce into a mathematical description of scattering two new quantities:

1. form factor, characterizes how single particle scatters;
2. structure factor, describes scattering due to spatial distribution of particles.

1.3 Principle of SAXS

SAXS is a x-ray scattering³ technique where the scattering of x-rays is recorded at low angles (typically $2\theta < 5^\circ$) (figure 2). This allows to probe the electron density distribution differences in length scales from nanometers to micrometers. Because of the small detection angle some requirements to the instrumentation follow up:

- extended sample-detector distance (L_{SD} , it is in range of meters);
- because interesting radiation is scattered under a small solid angle, there is possible to detect whole pattern simultaneously: two-dimensional detector needed;
- beamstop to prevent the direct incident beam damaging the detector.

³difference of scattering and diffraction is that in former case there is no long-range ordering in samples

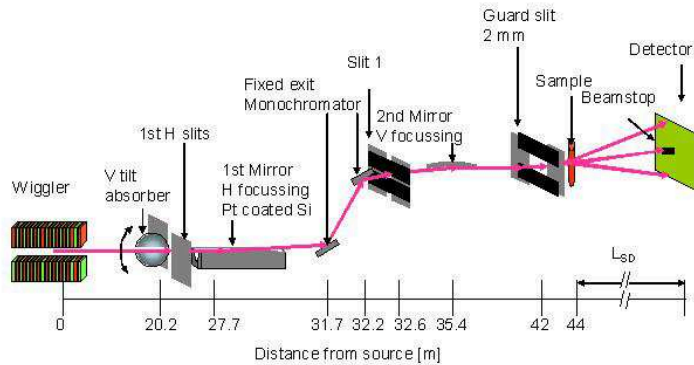


Figure 3: Schematic layout of beamline BW4.

2 Experiment

2.1 Samples

Investigated polymer PI-PEO has molar mass 9.708 kg/mol, 58 monomers in hydrophobic PI block and 131 monomers in hydrophilic PEO block. For measurements four samples were made with different water concentration (table 1). Samples were homogenized with intensive mechanical stirring in room temperature without heating. Corresponding concentration range was selected because it is known, that near 65% there is structure transition from hexagonally packed cylinders (HEX) to lamellae (LAM) [3].

Table 1: Samples.

sample code	actual water weigth %
PI-PEO-60	59.54
PI-PEO-65	64.96
PI-PEO-70	68.13
PI-PEO-75	74.61

2.2 SAXS experiment at beamline BW4

The beamline BW4 (figure 3) at DORIS III synchrotron at HASYLAB is dedicated to different x-ray scattering techniques. At BW4 the x-rays are produced by a wiggler, what determines the high flux and small divergence of the radiation. The x-ray beam is monochromatized using a fixed exit double

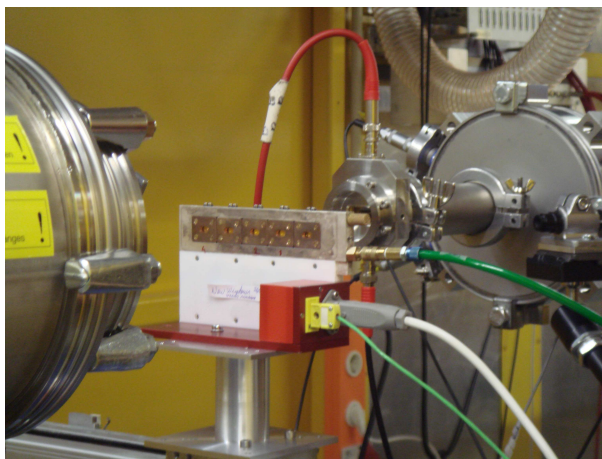


Figure 4: Sample cell used in measurements. This is specially constructed for SAXS measurements from soft matter and has heating and cooling options.

Si(111) monochromator and focused horizontally and vertically using a fixed cylindrical mirror and a plane mirror with a mirror bender respectively. The wavelength of radiation after monochromatization is 0.138 nm and it is hold fixed. Distance between the collimating slits (S1 and guard slit at figure 3) is about 10 m. Last 16 m of the beamline are inside the hutch and in there one can choose the sample position to change the L_{SD} . Each specific SAXS sample position requires the guard slit mounted close to the sample, to optimize the resolution and to reduce parasitic scattering. For this purpose the guard slit is portable. The blades of the guard slit are piezodriven. Between the guard slit and the sample there is a ionization chamber for beam monitoring. Scattered radiation is detected with a commercial 2D CCD detector (marCCD165), having chip area 2048×2048 pixels, each of $79.1 \mu\text{m}$ pixel size. The detective quantum efficiency for 10 keV photons is around 80%. The CCD chip is cooled down to -79°C , thus featuring a very low dark current. Close before detector there is rectangular lead beamstop with photodiode in the center to monitor the primary beam intensity. [4]

Measurements of the PI-PEO samples were conducted with the sample-detector distance 3850 mm (calculated from collagen pattern, the d-spacing of collagen is known). To measure temperature-dependence of samples special sample sell were used (figure 4). It has four cells for samples and one reference cell filled with water to measure the temperature. Pattern were detected at fallowing temperatures: 28°C , 35°C , 40°C , 50°C , 60°C , 70°C , 80°C and again at 28°C .

3 Results and analysis

3.1 Data processing

Because investigated samples are polycrystalline, the corresponding scattering pattern is isotropic. Only intensity dependence along the radius contains important information about the structure. So to make feasible analysis of the data, measured 2D scattering patterns were converted to 1D scattering curves (intensity versus modulus of the scattering vector $|\vec{q}| \equiv q$) in a way that regions affected by the beamstop were excluded. This was carried out with the program FIT2D⁴. Results are plotted in the figures 5–8. In all the samples one can see shifting of the peaks (Bragg's reflections) to higher q -values during heating. This indicates to the decreasing of the unit cell size. Samples PI-PEO-60 and PI-PEO-75 have HEX and LAM structures respectively (figures 5 and 8) [3]. In case of sample PI-PEO-65 one can clearly see continuous transition from HEX to LAM during the heating (figure 6). Sample PI-PEO-70 is a mixture of HEX and LAM structures, where most of the polymer has LAM structure (figure 7).

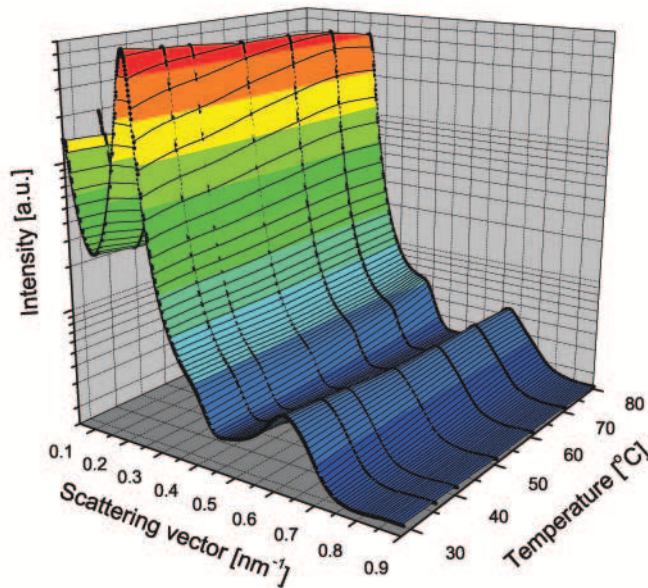


Figure 5: Temperature-dependence of scattering from sample PI-PEO-60.

⁴author: A. Hammersley, European Synchrotron Radiation Facility (ESRF)

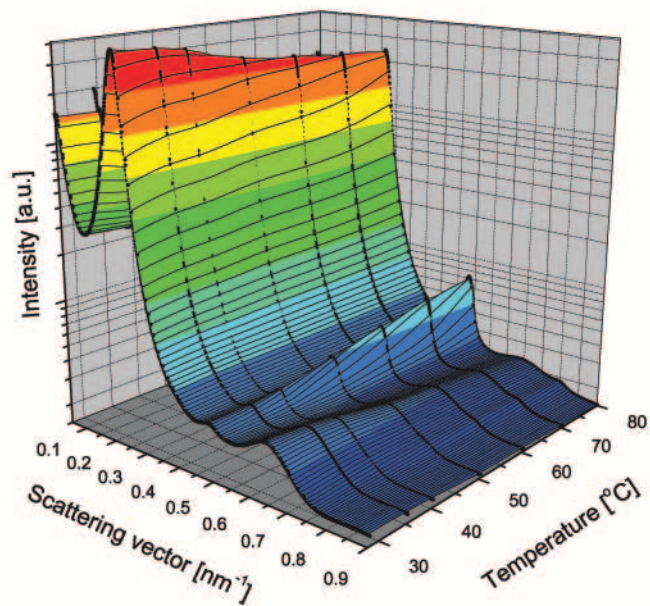


Figure 6: Temperature-dependence of scattering from sample PI-PEO-65.

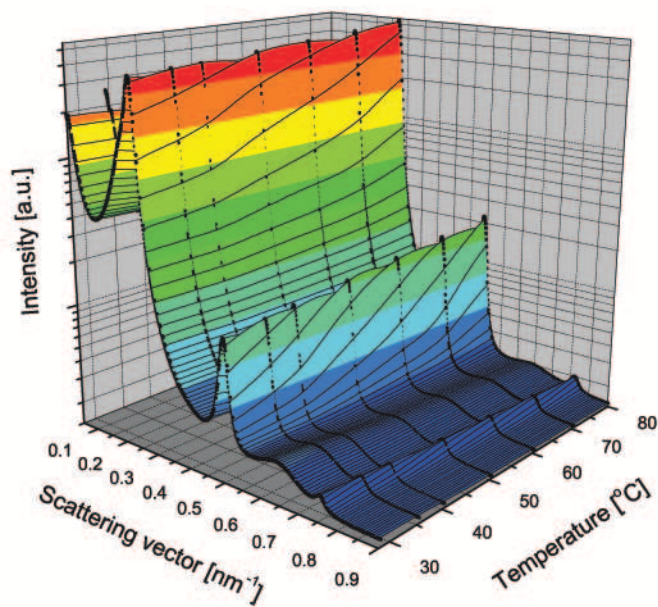


Figure 7: Temperature-dependence of scattering from sample PI-PEO-70.

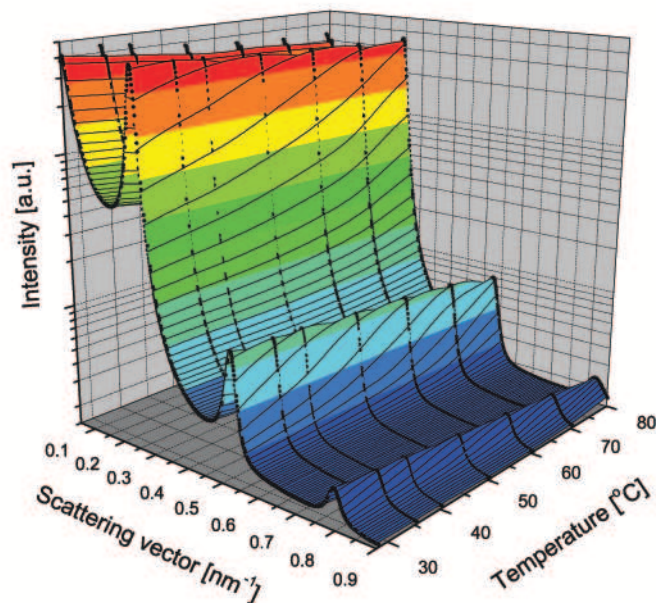


Figure 8: Temperature-dependence of scattering from sample PI-PEO-75.

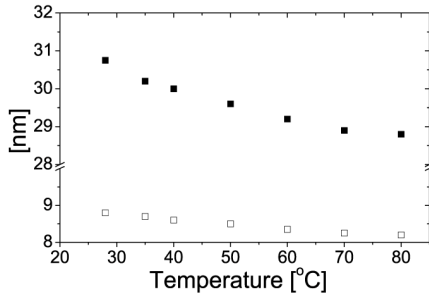
3.2 Data analysis

For modeling the data, special program named SCATTER⁵ were used [5] [6]. Examples from results can be seen on the figure 10. In the calculated curves are all features as in the measured curves, this indicates that the parameters of the model are in good agreement with the real structure. One can see deviation from experimental curves only in small q values in curves measured from the samples whit HEX structure, these errors are due to approximations in the model. Modeling was made with respect to:

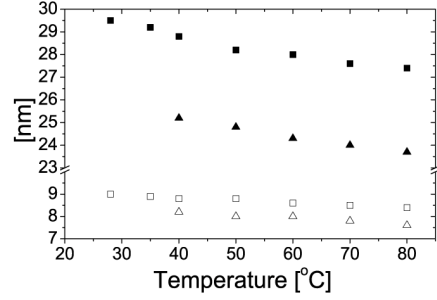
1. unit cell length (position of the Bragg's reflections);
2. polyisoprene particle radius (radius of a cylinder or half-thickness of a lamella, affects positions of minimums of a form factor oscillations);
3. relative proportion of HEX and LAM structures (only in case of PI-PEO-65 and PI-PEO-70).

To get the curves over one another and look more accurate some more parameters were varied:

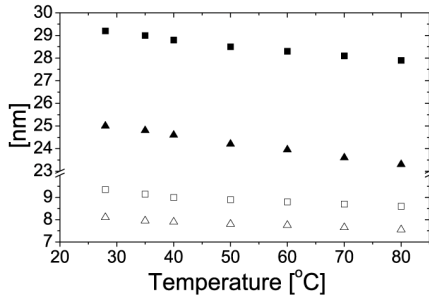
⁵author: S. Förster, University of Hamburg, http://www.chemie.uni-hamburg.de/pc/sfoerster/software_e.html



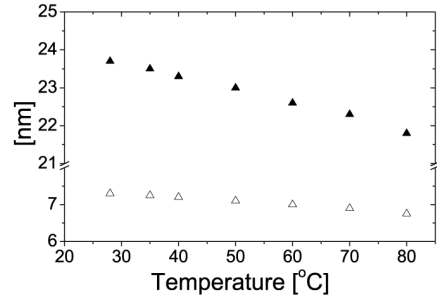
(a) PI-PEO-60



(b) PI-PEO-65



(c) PI-PEO-70



(d) PI-PEO-75

Figure 9: Temperature-dependence of relevant structural parameters. Filled boxes and triangles mark unit cell length of HEX and LAM structures respectively. Empty boxes and triangles mark particle radius of HEX and LAM structures respectively.

- standard deviation of a particle radius (particle polydispersity);
- average size of a crystal domains;
- standard deviation of a unit cell length;
- baseline intensity;
- arbitrary proportionality factor.

In all calculated curves peaks have Lorentzian shape. Temperature-dependences of unit cell lengths and particle radiuses are plotted on figure 9.

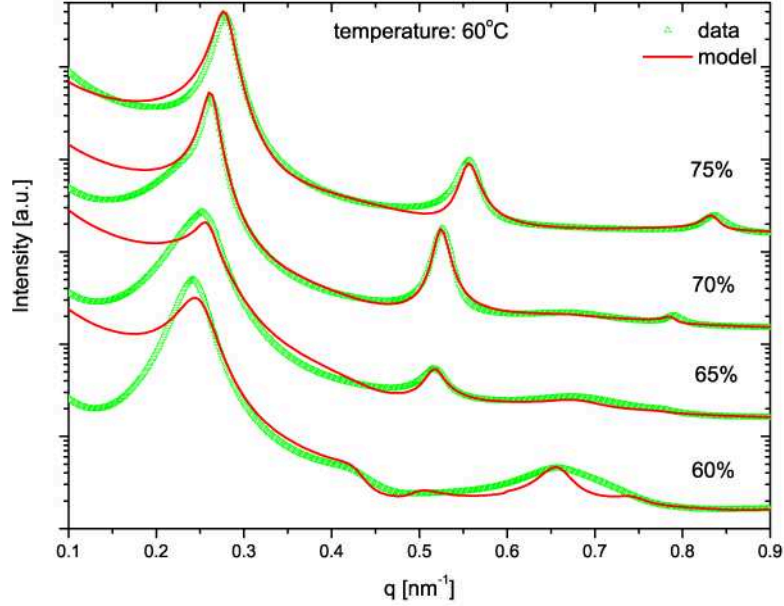


Figure 10: Measured curves compared with calculated curves.

3.3 Comparison of structures before and after heating

As one can see from the scattering curves (figure 11) in all samples were noticeable structural changes after heating (table 2). In sample PI-PEO-60 unit cell length and cylinder radius are slightly bigger then before. When in sample PI-PEO-65 has before heating pure HEX structure, then after temperature treatment there is a mixture of HEX and LAM. Also the structural parameters of HEX structure are smaller. In sample PI-PEO-70 only the relative proportion of different structures changes. In case of PI-PEO-75 unit cell length and thickness of lamellae are smaller then before.

Table 2: Comparison of structure parameters before and after heating.

sample code	structure	unit cell length [nm]		particle radius [nm]	
		before	after	before	after
PI-PEO-60	HEX	30.75	31.35	8.8	8.9
PI-PEO-65	HEX	29.5	29.25	9	8.9
	LAM	-	25.5	-	8
PI-PEO-70	HEX	29.2	29.2	9.35	9.3
	LAM	25	25	8.1	8.1
PI-PEO-75	LAM	23.7	23	7.3	7

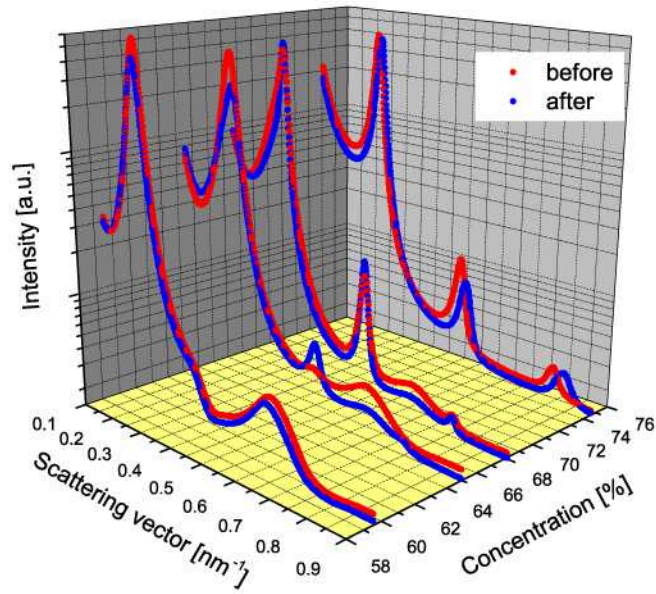


Figure 11: Comparison of measured scattering curves before and after heating.

4 Summary

In all investigated samples decreasing of the unit cell length and particle radius during heating were found. One possible explanation to this phenomena is the rearrangement of the solvent (water) molecules. In sample PI-PEO-65 temperature induced structure transition from HEX to LAM were discovered.

Because the structure of the samples are different before and after heating, one can conclude that before heating samples are in non equilibrium state. Intriguingly the affect of the temperature treatment is different in all samples.

References

- [1] A. K. Khandapur, S. Förster, F. S. Bates, I. W. Hamley, A. J. Ryan, W. Bras, K. Almdal, K. Mortensen, “Polyisoprene-Polysyrene Diblock Copolymer Phase Diagram near the Order-Disorder Transition,” *Macromolecules* 28, 8796–8806 (1995).
- [2] N. Stribeck, *X-Ray Scattering of Soft Matter* (Springer, Berlin, 2007).
- [3] A. Timmann, “Untersuchung des lyotropen Phasenverhaltens und der Solubilisierung von Polyiopren-block-polyethylenoxid-copolymeren mittels Röntgenkleinwinkelstreuung,” Ph.D. thesis, University of Hamburg (2005).
- [4] S. V. Roth, R. Döhrmann, M. Dommach, M. Kuhlmann, I. Kröger, R. Gehrke, H. Walter, C. Schroer, B. Lengeler, P. Müller-Buschbaum, “Small-angle options of the upgraded ultrasmall-angle x-ray scattering beamline BW4 at HASYLAB,” *Rev. of Scientific Instr.* 77, 085106 (2006).
- [5] S. Förster, A. Timmann, M. Konrad, C. Schellbach, A. Meyer, S. S. Funari, P. Mulvaney, R. Knott, “Scattering Curves of Ordered Mesoscopic Materials,” *J. Phys. Chem. B* 109, 1347–2360 (2005).
- [6] S. Förster, C. Burger, “Scattering Function of Polymeric Core-Shell Structures and Excluded Volume Chains,” *Macromolecules* 31, 879–891 (1998).